A Consistent Prescription of Stratospheric Aerosol for Both Radiation and Chemistry in the Community Earth System Model (CESM1)

R. R. Neely III[1,2*], A. Conley[2], F. Vitt[2], J.F. Lamarque[2]

[1] {National Centre for Atmospheric Science (NCAS) and the School of Earth and Environment (SEE), University of Leeds, Leeds. United Kingdom}

[2] {National Center for Atmospheric Research (NCAR), Boulder, Colorado}

Correspondence to: R. R. Neely III (R.Neely@leeds.ac.uk)

Abstract

Here we describe an updated parameterisation for prescribing stratospheric aerosol in the National Center for Atmospheric Research (NCAR) Community Earth System Model (CESM1). The need for a new parameterisation is motivated by the poor response of the CESM1 (formerly referred to as the Community Climate System Model, version 4, CCSM4) simulations contributed to Coupled Model Intercomparison Project 5 (CMIP5) to colossal volcanic perturbations to the stratospheric aerosol layer (such as the 1991 Pinatubo eruption or the 1883 Krakatau eruption) in comparison to observations. In particular, the scheme used in the CMIP5 simulations by CESM1 simulated a global mean surface temperature decrease that was inconsistent with the GISS Surface Temperature Analysis (GISTEMP), NOAA's National Climatic Data Center and the Hadley Centre of the UK Met Office (HADCRUT4). The new parameterisation takes advantage of recent improvements in historical stratospheric aerosol databases to allow for variations in both the mass loading and size of the prescribed aerosol. An ensemble of simulations utilizing the old and new schemes show CESM1's improved response to the 1991 Pinatubo eruption. Most significantly, the new scheme more accurately simulates the temperature response of the stratosphere due to local aerosol heating. Results also indicate that the new scheme decreases the global mean temperature response to the 1991 Pinatubo eruption by half but observed, and modelled climate variability preclude statements as to the significance of this change.

1 Introduction

Volcanic perturbations to the stratospheric aerosol layer are an often ill represented forcing in the climate model simulations (Solomon et al., 2011; Driscoll et al., 2012; Knutson et al., 2013; Zanchettin et al. 2015; Kremser et al., 2016). Earth's climate system has been perturbed by several colossal (volcanic explosivity index (VEI) of 5 or greater) volcanic eruptions since 1960 (see Figure 1) (Newhall and Self 1982). The impact each of these eruptions has had on the global mean surface temperature anomaly is shown in Figure 1.

Figure 1 compares the Coupled Model Inter-comparison Project 5 (CMIP5) multi-model global mean surface temperature anomaly to three different observationally based datasets (Taylor et al. 2012). The vertical dashed grey lines note the date of colossal volcanic perturbations accounted for in most of the forcing files utilized in the CMIP5 simulations. Figure 1 shows that the response of the Nation Center for Atmospheric Research's (NCAR) Community Climate System Model, version 4 (CCSM4) (now referred to as the NCAR Community Earth System Model (CESM1)), highlighted in red, to volcanic forcing, as well as the response of most other models submitted to CMIP5.

Stratospheric aerosol is prescribed in several ways with various levels of complexity in global climate models. Most models contributing to CMIP5, including CCSM4/CESM1 (Meehl et al. 2012), prescribed a zonal mean, monthly mean stratospheric aerosol mass or stratospheric aerosol optical depth (SAOD) as well as the surface area density (SAD) of the aerosol (using datasets such as Sato et al. (1993), Stenchikov et al. (1998) or Ammann et al. (2003)). Typically this specification of aerosol is ingested within the model's 1) radiative transfer parameterisation and 2) chemistry parameterisation using several underlying assumptions about the size distribution and composition of the aerosol. Though adequate, these methods leave much to be desired for accurately simulating the evolution of the perturbation to the stratospheric aerosol layer after these eruptions.

To address the need for a more accurate representation of colossal volcanic eruptions in the atmospheric current climate models, including all the configurations of the Community Atmosphere Model (CAM) and Whole Atmosphere Community Climate Model (WACCM) within the framework of the CESM1 (Lamarque et al. 2012; Neale et al. 2013; Marsh et al. 2012; Meehl et al. 2013), a new dataset was derived to force models participating in the Chemistry Climate Model Initiative (CCMI) (Eyring and Lamarque, 2012; Eyring et al.

2013). Here we describe the implementation of this dataset in CESM1 with additional updates in preparation for CCMI Phase 1 simulations (Eyring et al., 2013).

In Sections 2, 3 and 4 we discuss the original prescriptions of stratospheric aerosol in all configurations of CESM1. Section 5 discusses the new stratospheric aerosol prescription for all of CESM1. Table 1 summarises the main similarities and differences between the old and new parameterizations described in Section 2 through 5. In Section 6 we describe the behaviour of CESM1 and response of the model to the new representation of the 1991 Pinatubo eruption. In Section 7 we summarise our work and make suggestions for future use of this new stratospheric aerosol scheme in CESM1.

2 Summary of Original CCSM4/CESM1 Dataset and Implementation

Previous to CESM1, CESM1(CAM4) was part of CCSM4. Neale et al. (2010) describe the scheme used to specify volcanic eruptions and the stratospheric aerosol layer in CCSM4 (specifically with in CAM4.0) and how this interacts with the other parameterizations of the model. For a description of the model's climate and its response to forcings see Meehl et al. (2012). Here we summarize the main features of the volcanic prescription in CCSM4/ CESM1(CAM4) that have been changed significantly in the updated scheme described below so that future studies utilizing CESM1 may account for changes in the model's behaviour compared to simulations conducted for CMIP5.

In CCSM4/ CESM1(CAM4), stratospheric aerosol is treated by prescribing a single zonally averaged species. The prescription consists of a monthly-mean mass (kg/m^2) distributed on a predefined meridional and vertical grid. The input time series from 1850 to 2010 is based upon Ammann et al. (2003). This aerosol mass is assumed to be comprised of 75% sulphuric acid and 25% water and have a constant log-normal size distribution with a wet effective radius (r_{eff} i.e. the third moment divided by the second moment of the size distribution) of 0.426μm and a standard deviation (σ(ln r)) of 1.25. The standard CCSM4/CESM1(CAM4) forcing file is entitled "CCSM4_volcanic_1850-2008_prototype1.nc" and may be found on the CESM input data repository at "/glade/p/cesm/cseg/inputdata/atm/cam/volc/".

In CCSM4/CESM1(CAM4) the stratospheric aerosol mass is interpreted by the radiative transfer code via the predefined mass-specific extinctions, single scattering albedos, and asymmetry parameters. These parameters are calculated using the constants defined above and are stored in lookup tables for the shortwave and long wave radiative transfer schemes separately (the table has a single dimension that varies by spectral band) for use by each of

the spectral bands in the Community Atmosphere Model Radiative Transfer (CAMRT) parameterization. The optical property file for CCSM4/CESM1(CAM4) is entitled "sulfuricacid_cam3_c080918.nc" and may be found on the CESM input data repository at "/glade/p/cesm/cseg/inputdata/atm/cam/physprops/". This information is combined with similar information from other radiatively active species in CCSM4/CESM1(CAM4) as specified by Neale et al. (2010).

3 Summary of Original CESM1(CAM5) Dataset and Implementation

Here we summarize the main features of the stratospheric aerosol prescription in CESM1(CAM5) so that differences may be accounted for between future simulations using the new CESM1 stratospheric aerosol scheme and previous simulations conducted for CMIP5. For a discussion of the parameterisation used to represent stratospheric aerosol in CESM1(CAM5) please see chapter 4 of Neale et al. (2012).

CESM1(CAM5) specifies the stratospheric aerosol as a mass mixing ratio of wet sulphate aerosol (i.e. a mixture of 75% sulphuric acid and 25% water) to dry air as a function of height, latitude and time. Unlike CCSM4/CESM1(CAM4), CESM1(CAM5) has the ability to include non-zonally symmetric aerosol (i.e. varying by longitude). In the update described below, this ability has been spread to all present configurations of CESM1.

CESM1(CAM5) utilises the Rapid Radiative Transfer Method for GCMs (RRTMG) (Mlawer et al., 1997; Iacono et al., 2008). For each short-wave band calculation, extinction optical depth, single scattering albedo and asymmetry factors are determined from the aerosol properties according to their size and mass and radius. For each long-wave band only absorption optical depth is calculated.

As with CCSM4/CESM1(CAM4), to interact with the radiative transfer scheme, CESM1(CAM5) calculates mass-specific properties over each spectral band of RRTMG. The calculations assume the size distribution of the aerosol to be a log-normal distribution with a geometric mean radius r_g, that is allowed to vary as specified by the aerosol forcing file, and a constant geometric standard deviation σ_g, specified as a constant 1.8 within the assumptions that are used to form the optical parameters file. The results of the calculations are stored in a lookup table with both $\mu = \ln(r_g)$ and the RRTMG spectral bands as independent variables. This is the main difference between the CCSM4/CESM1(CAM4) and CESM1(CAM5) when

it comes to representing the impact of stratospheric aerosols. Instead of a one-dimensional look up table (i.e. just varying over spectral band) as CAMRT uses in CCSM4/CESM1(CAM4), RRTMG utilizes a two-dimensional look up table that varies by μ and spectral band. The lookup table is entitled "rrtmg_Bi_sigma1.8_c100521.nc" and may be found on the CESM input repository at "glade/p/cesm/cseg/inputdata/atm/cam/physprops/"

Note that for a log-normal distribution, the geometric mean radius (r_g) and the median (r_m) are equal and the effective radius is related to the geometric radius and geometric standard deviation by $r_{eff} = r_g \exp\left(\frac{5}{2}\left(\ln\sigma_g\right)^2\right)$. The geometric standard deviation is the exponential of the standard deviation of ln*(r)* (See Grainger (2015) for derivations of log-normal aerosol size distribution properties.).

In CESM1(CAM5) the mass-specific aerosol extinction, scattering, and asymmetry factor are defined as:

$$b_{ext} = \frac{3}{4\rho r_{eff}} \int_0^\infty Q_{ext}(r) dL(r) \quad (1)$$

$$b_{sca} = \frac{3}{4\rho r_{eff}} \int_0^\infty Q_{sca}(r) dL(r) \quad (2)$$

$$b_{asm} = \frac{3}{4\rho r_{eff}} \int_0^\infty Q_{asm}(r) dL(r) \quad (3)$$

The mass-specific absorption is defined as the difference of the extinction (Equation 1) and scattering (Equation 2):

$$b_{abs} = \frac{3}{4\rho r_{eff}} \int_0^\infty \left(Q_{ext}(r) - Q_{sca}(r)\right) dL(r) \quad (4)$$

Where $L(r)$ is the incomplete gamma function defined as

$$L(r) = \int_0^r r^{*2} n(r^*) dr^* \,/\, \int_0^\infty r^{*2} n(r^*) dr^* \quad (5)$$

and the density (ρ) of the assumed 75%/25% sulphuric acid to water mixture at 215K is 1750 kg/m^3. $Q_{ext}(r)$, $Q_{sca}(r)$, $Q_{asm}(r)$ are the Mie efficiencies parameters obtained from the MIEV0 software (Wiscombe, 1996).

Similar to CCSM4/CESM1(CAM4), the standard configuration of CESM1(CAM5) uses the stratospheric aerosol forcing dataset over the period 1850 to 2010 from Ammann et al. (2003). This dataset does not take advantage of the parameterisation in CESM1(CAM5), as described above, to modulate the changes in stratospheric size distribution (i.e. variations in r_g as

described above). Instead, similarly to CCSM4/CESM1(CAM4), the mass from the Ammann et al. (2003) dataset is assumed to be comprised of 75% sulphuric acid and 25% water and have a constant log-normal size distribution with a wet effective radius of 0.426μm and a standard deviation (σ(ln r)) of 1.8. It should also be noted that the Ammann et al. (2003) is a zonally averaged dataset and, therefore, does not take advantage of CESM1(CAM5)'s ability to utilize a zonally asymmetric forcing file. The standard CESM1(CAM5) forcing file is entitled "CCSM4_volcanic_1850-2008_prototype1.nc" and may be found on the CESM input data repository at "/glade/p/cesm/cseg/inputdata/atm/cam/volc/".

4 Summary of Original CESM1(WACCM4) and CESM1(CAM4-chem) Dataset and Implementation

In CESM1(WACCM4) and CESM1(CAM4-chem), the prescription of stratospheric aerosol differs from CCSM4/CESM1(CAM4) and CESM1(CAM5) due to the need to specify SAD for use in the heterogeneous stratospheric chemistry parameterization. Marsh et al. (2013), building upon Tilmes et al. (2009), describe the CESM1(WACCM4) scheme. For details about CESM1(CAM4-chem) see Lamarque et al. (2012). In both model configurations, the SAD is prescribed from a monthly zonal-mean time series derived from observations and is identical to that specified in the CCMVal2 REF-B1 simulations (Eyring et al. 2010; SPARC CCMVal, 2010). The standard SAD input file is "/glade/p/cesm/cseg/inputdata/atm/waccm/sulf/SAD_SULF_1849-2100_1.9x2.5_c090817.nc".

The mass of aerosol to be used by CAMRT (which is the standard radiative transfer model used in both model configurations) is derived from the specified SAD by determining a volume density of sulphate aerosol by assuming a lognormal size distribution with fixed size (r_{eff} = 0.5μm), standard deviation (σ(ln r))=1.25) and number density (Kinnison et al. 2007). The mass of aerosol per unit volume is the derived using the ratio of H_2O to H_2SO_4 within each aerosol droplet as parameterized by Tabazadeh et al. (1997). This differs from CCSM4/CESM1(CAM4)'s and CESM1(CAM5)'s assumed aerosol composition of 75% sulphuric acid and 25% water. However, the optical constants in the radiation parameterisation still assume this composition. The exact same optical property file for CCSM4/CESM1(CAM4) is by CESM1(CAM4-chem) and CESM1(WACCM4) and, again, is entitled "sulfuricacid_cam3_c080918.nc" and may be found on the CESM input data repository at "/glade/p/cesm/cseg/inputdata/atm/cam/physprops/". Besides the determination

of mass described above from the SAD input file, the parameterisation of stratospheric aerosol in CAMRT in CESM1(WACCM4) and CESM1(CAM4-chem) is the same as in CCSM4/CESM1(CAM4).

5 Implementation of the New Prescribed Stratospheric Aerosol Scheme in CESM1

In this work, we have unified the stratospheric aerosol parameterisation for CESM1(CAM4) and CESM1(CAM4-chem) (both found within NCAR's CESM1 code repository under tag cesm1_1_1_ccmi23), CESM1(WACCM4) and CESM1(CAM5) (both of the latter configurations found within the CESM1 repository under tag cesm1_1_1_ccmi30) to take advantage of the new forcing data prepared for the CCMI simulations (Eyring et al., 2013). The new forcing file is derived from the SAGE 4λ dataset that is described by Arfeuille et al. (2013). The main advantage is that the new dataset includes information on the mass, size and SAD that are all derived from a coherent set of observations and modelling assumptions.

Here we only describe the changes made to the CESM1's configurations. For the more detailed documentation of CAMRT (the radiation scheme in CESM1(CAM4), CESM1(CAM4-chem) and CESM1(WACCM4)) and RRTMG (utilised in CESM1(CAM5)), which were not modified here, please see Neale et al. (2010; 2012) as noted above. In summary, three main changes occurred: 1) the forcing input file (this has the main advantage of updating the stratospheric aerosol masses to reflect the most current observational and modelling studies as well as providing a coherent dataset of aerosol mass, surface area density and radius), 2) CAMRT has been modified to allow for variations in the effective radius of the aerosol distribution with time as provided by the new forcing file and 3) the optical look up tables for both CAMRT and RRTMG were updated with new Mie calculations for use in all model configurations.

5.1 Forcing File

For the new implementation of the stratospheric aerosol forcing in CESM1 we utilize the new stratospheric aerosol dataset derived to force models participating in CCMI (Eyring et al. 2013). The CCMI stratospheric aerosol forcing file (the data and more detailed description are available from http://www.pa.op.dlr.de/CCMI/CCMI_SimulationsForcings.html) was chosen as a basis for the CESM1 stratospheric aerosol parameterisation update as it provides updated values of aerosol mass loading as well as temporally and latitudinally varying values for the size and SAD of the aerosol distribution. Thus, the information contained in this dataset can

be used by the new stratospheric aerosol parameterisation in conjunction with both CESM1's radiative and chemical schemes. This is a significant improvement upon the separate datasets utilised in previous versions of CESM1.

The original CCMI stratospheric aerosol forcing file provides the mass loading, SAD and size of aerosol from 1960 to 2012. The original file was modified slightly to form the new standard input file for CESM1 for period ranging from 1950 to 2012. The current CCMI forcing file is entitled "CESM_1949_2100_sad_V2_c130627.nc" and can be found on the CESM input data repository. The main difference between this file and the original file is that the monthly-mean values from the minimum in stratospheric aerosol observed in 1998 and 1999 have been used to fill in the years from 1949 to 1959 and into the future from 2012 to 2100. This was done in accordance with the assumptions and scenarios laid out by the CCMI specification (Eyring et al. 2013).

To enable simulations prior to 1960, an additional forcing file is available entitled "CESM_1849_2100_sad_V3_c160211.nc". This file is identical to the "CESM_1949_2100_sad_V2_c130627.nc" from 1960 to 2100. Previous to this period (i.e. from 1849 to 1960) we have added the impact of colossal volcanic eruptions (VEI 5 and larger) and a representation of the background stratospheric aerosol layer. For this period, we have included the following 7 colossal volcanic perturbations to the background stratospheric aerosol layer: 1) Sheveluch in February 1854, 2) Krakatau in May 1883, 3) Okataina in June 1886, 4) Santa Maria in October 1902, 5) Ksudach in March 1907, 6) Novarupta in June 1912 and 7) Bezymianny in October 1955. In between the eruptions, background levels of stratospheric aerosol are based on the monthly-mean mass and size from the minimum in stratospheric aerosol observed in 1998 and 1999 (as done for the 1949 to 2100 period described above).

The volcanic perturbations were included in the forcing file by scaling the aerosol mass, size and SAD of the Pinatubo eruption from 1991 to 1998 eruption according to the ratio of injected mass SO_2 of the desired eruption to that observed for 1991 Mt. Pinatubo eruption. Aerosol mass was scaled directly while radii were scaled by the one third power of the injection ratio and SAD were scaled by the two thirds power of the injection ratio. We admit that this is a crude estimate of the eruption impact but is in line with methods used for previous databases (such as using datasets such as Ammann et al. (2003) and Sato et al. (1993)).

To implement the use of the new stratospheric input file in CESM1, several modifications were made to the mechanics of how the CESM1 ingests stratospheric aerosol forcing files so that time varying information about the size of the aerosol could be included within the radiative calculations. This resulting code, entitled "prescribed_strataero.F90" is located in the chemistry utilities of CESM ({top level directory of model version}/models/atm/cam/src/chemistry/utils/prescribed_strataero.F90). This code reads the necessary input parameters and transforms them into the units and grid needed by the model configuration. By default, it also masks out any aerosol below the model's tropopause. This is and option that may easily be changed. The code may also be easily modified and adapted to input values from other input files.

It should be noted that CESM1 linearly interpolates the input file in time and space to match the time step and spatial grid of the model configuration. As such, this results in differences between the monthly mean aerosol specified from the ingested forcing file and monthly mean values of the aerosol that the model actually experiences. This is particularly an issue during periods of rapid change in aerosol. Similar issues have been noted for the specification of ozone in Neely et al. (2014). The best method to counteract errors due to this issue is to specify the aerosol values at the highest temporal cadence available.

5.2 Optical Properties

As in previous versions of the model, here we assume that the stratospheric aerosol is comprised of a mixture of 75% sulphuric acid and 25% water and conforms to a log-normal size distribution. Unlike the previous parameterizations, the distribution has a varying effective radius that is specified by the input file.

As described above, CESM1(CAM5) already provided the necessary mechanism to use the temporally and latitudinally varying aerosol size information from the input file. For CESM1(CAM4), CESM1(CAM4-chem-CCMI) and CESM1(WACCM4-CCMI) we adapted the shortwave mechanism of CESM1(CAM5) to use both mass and r_g to look up the mass-specific aerosol extinction, scattering, and asymmetric scattering for each of CAMRT's shortwave bands. In doing so, a new optical properties file was determined for all configurations of CESM1(CAM4) and CESM1(WACCM4) (i.e. all configurations of CESM1 that utilise CAMRT) to allow for the variations in r_g. This file is entitled "volc_camRT_byradius_sigma1.6_c130724.nc" and is available for download from the

CESM input data repository (access is described below) in the physics properties folder of CAM (/trunk/inputdata/atm/cam/physprops/volc_camRT_byradius_sigma1.6_c130724.nc).

To create the new optical lookup table for CAMRT, a new set of Mie efficiency terms was determined for a range of wavelengths and size parameters appropriate for the CAMRT and the new aerosol input file. The index of refraction used in these calculations is based on the assumption of a 75% to 25% mixture of sulphuric acid and water at 293K. Data for this was compiled from the GEISA spectroscopic database (http://ether.ipsl.jussieu.fr). The specific data used was originally reported by Biermann et al. (2000). The data file used in the optical calculations is entitled "volcsulfrefind75-25.mat" and is available by contacting the lead author. The file is organized by the real and imaginary parts of the index of refraction and contains both the original data and fit parameters used to create the final data set that evenly spans the desired spectrum region. The parameters used in the final Mie calculation are 'realind', 'imind', 'realmicron' and 'immicron'.

All Mie calculations were done using the "MATLAB Functions for Mie Scattering and Absorption" developed by Mätzler (2002). The code used to create the CAMRT optical properties may be found in section S1 of the supplement.

A similar method was used to also update the optical properties file for all configurations of CESM1 that utilise RRTMG (i.e. CESM1(CAM5). The new optical properties file for model configurations using RRTMG is entitled "volc_camRRTMG_byradius_sigma1.6_c130724.nc" and is available from CESM's input data repository (/trunk/inputdata/atm/cam/physprops/ volc_camRRTMG_byradius_sigma1.6_c130724.nc). This code is attached in supplement section S2. The main difference between the two versions of the code are the spectral bands of the two radiative transfer schemes. This is a direct consequence of the different bands used by CAMRT versus RRTMG. In addition, only the shortwave parameters were updated for the CAMRT files while both the shortwave and longwave were updated in RRTMG files. The reason for only adjusting the shortwave parameters in CAMRT are purely historical due to the complex entanglement of the different species in the longwave parameterisation CAMRT. It was also thought that little improvement would have been made to the model's response to perturbations to the stratospheric aerosol layer.

6 Results from the New CESM1 Stratospheric Aerosol Parameterisation

In Figure 2 we document the resulting global SAOD between 1960 and 2000 produced by the new prescribed stratospheric aerosol parameterisation utilising forcing entitled "CESM_1949_2100_sad_V2_c130627.nc" (referred to as the new CESM1 AOD). This is in comparison to the SAOD resulting from the parameterisation used by the original CCSM4/CESM1 and the latest version of the observationally based Sato et al. (1993) dataset. Several differences are apparent in the comparison. In general, the peak global mean SAOD after each major eruption is reduced in the new CESM1 compared to both the original CCSM4/CESM1 specification and the AOD of the Sato et al. (1993) dataset. The one exception to this is the 1963 Agung eruption in which the Sato et al. (1993) results show an even more reduced, though broader, peak than both the original CCSM4/CESM1 and new CESM1. Between the Agung eruption in 1963 and the 1974 Fuego eruption, there are many significant differences between the three SAOD time series. Notably, the CESM1 SAOD does not peak in 1968 as the other two data do and the Sato et al. (1993) show higher levels of aerosol throughout the period. The reasons for these differences are due to the underlying assumptions about the eruptions included in the creation of the forcing file. Though several moderate eruptions (VEI 4) are known to have occurred in this period (Stothers 2001; Bauer 1979; Hofmann et al. 1992; Langmann 2013; Sato et al. 1993), measurements are sparse and, without further investigation, the correct representation of these perturbations to the stratospheric aerosol burden is highly uncertain. After Fuego, outside of periods perturbed by volcanic eruptions, Sato et al. (1993) and new CESM1 display similar levels of background SAOD while the CCSM4/CESM1 does not account for background stratospheric aerosol (the impact of this exclusion of background stratospheric aerosol is discussed in Solomon et al. (2011)).

Figure 3 examines the differences between the new and old prescribed stratospheric aerosol schemes in more detail. Figure 3 shows a comparison of the resulting monthly mean, zonal mean SAOD after the 1991 Mt. Pinatubo eruption from old and new schemes in CESM1(CAM4) (panels a & b) and CESM1(CAM5) (panels c & d). Figure 3 shows that, to first order, the most significant change in the new scheme is the distribution of mass used in the forcing file. For further examination of the impact of the individual changes to the radiation code and forcing file on CESM1(CAM4) and CESM1(CAM5) see section S3 of the supplement. Results for CESM1(WACCM4) and CESM1(CAM4-Chem) are not shown as the

new stratospheric aerosol are identical to those utilised in the new CESM1(CAM4) prescription.

To examine the impact of the new stratospheric forcing on CESM1's simulated climate response, we performed an experiment that compared 5 ensemble members of CESM1(CAM5) with the new stratospheric aerosol parameterisation versus 5 members using the original parameterisation over the period influenced most strongly by 1991 Mt. Pinatubo eruption. Each of the 5 members in the respective ensembles used different initial ocean states and atmospheric initial conditions that were derived from the original five CESM1(CAM5) CMIP5 simulations. The differences between the two ensembles shows the possible improvement the new scheme has on CESM1's ability to simulate the climate response to a colossal volcanic eruption.

In Figure 4 we show the impact on the simulated global monthly mean top of atmospheric net radiative flux. A reduction is seen at the peak of the stratospheric aerosol perturbation in late 1991. Notably, outside the period of highest aerosol loading after the eruption (i.e. the second half of 1991), there is very little difference in the net radiative flux between the two ensembles.

In Figure 5, the global annual mean temperature (i.e. the response to the differences in the simulated forcings in Figure 4) is shown for each of the 2 ensembles in comparison to observations from the GISS Surface Temperature Analysis (GISTEMP) (Hansen et al., 2010; GISTEMP Team, 2015). For the original CCSM4/CESM1 forcing parameterization, the difference between the model and analysis record is similar to Figure 1 while the new parameterisation simulates a trend that more closely follows the observed record within the variability of the model runs and error estimate of the observations. The most significant improvement is observed in the 1992 global annual temperature. As in Figure 1, the original CCSM4 parameterisation causes the simulated ensemble mean, global mean temperature anomaly to drop ~0.4°C in 1992. This is double decrease in temperature shown in the GISTEMP record (~2 x 0.2°C), and at upper end of the published estimates (Thompson et al. 2009; Canty et al. 2013; see below). In comparison, the ensemble using the new parameterisation suggests a decrease in ensemble mean global mean temperature of ~0.25°C, though the variability of completely over laps with the reported observational range. Beyond 1992, GISTEMP and the two ensembles produce results that agree within the observed and simulated climate variability.

Note that the observed global mean temperature in 1991 contains a strong ENSO signal (Thompson et al. 2009; Canty et al. 2013), which the model ensemble will not accurately reproduce due to its own inherent variability. This causes significant difficulty in the use of changes in global mean temperature as a metric for model improvement after the 1991 Pinatubo eruption. Studies that have attempted to isolate the pure volcanic surface cooling signal from other sources of variability (including ENSO) result in estimates of maximum cooling ranging from ~0.14°C to ~0.4°C (Thompson et al., 2009; Canty et al., 2013). Thus, the CESM1's global mean temperature response to the 1991 Pinatubo eruptions resulting from both the old and new stratospheric aerosol parameterizations are within the uncertainty range of observation-based estimates. Fully, demonstrating the improvement of CESM1's global mean temperature response to colossal volcanic eruptions is beyond the current scope of this work due to the computing necessary to create a large enough ensemble of runs (perhaps >40 of each parameterisation given the variability seen in CESM's Large Ensemble (Kay et al. 2015) to accurately estimate model variability.

In addition to the changes in the global surface temperature response, the new stratospheric aerosol scheme drastically improves the CESM1(CAM5)'s performance in representing stratospheric heating after a colossal volcanic eruption. This is shown in Figure 6 where we compare the 50hPa temperature anomaly for the two ensembles against the Radiosonde Innovation Composite Homogenization (RICH) (Haimberger et al., 2008). This is notable as the original stratospheric aerosol scheme in CCSM4/CESM1 caused heating that was over seven times the observed anomaly and had significant implications for changes in stratospheric dynamics and chemistry. In the new CESM1 scheme, the simulated stratospheric heating is at most double the observed anomaly.

7 Summary

Here we describe the new prescribed stratospheric aerosol parameterisation for CESM1. This work represents a significant improvement in the prescribed representation of stratospheric aerosols in CESM1 as it unifies the treatment between the chemical and radiative transfer parameterizations within all atmospheric models under the CESM1 umbrella. We have shown that the new prescription of stratospheric aerosol consistently improves the representation of stratospheric aerosol and resulting model response, especially after colossal volcanic eruptions. Most significantly, the new scheme more accurately simulates the stratospheric

temperature response to the 1991 Pinatubo eruption. Results also indicate that the new scheme decreases CESM's global mean temperature response but observed and modelled climate variability preclude statements as to the significance of this improvement.

This scheme may also be easily adapted to other stratospheric aerosol forcing scenarios, such as those used in geoengineering experiments, by simply changing the masses, radii and SAD of the input file as has been done in Xia et al. (2016). For future historical simulations, there are two possible new prescribed stratospheric aerosol datasets being prepared for CMIP6 that the new CESM1 parameterisation will be able to utilise. One will be an update to the CCMI dataset presented here that covers the period form 1850 to present. The second file will be created using the output of a prognostic stratospheric aerosol scheme within CESM1 (Mills et al. 2016) that simulates the stratospheric aerosol layer from 1850 to present day and uses only the injections of SO2 from the VolcanEESM (Neely and Schmidt 2016) database.

Here we have focused on the technical specification of the new implementation of prescribed stratospheric aerosol in CESM1 and the impact this new specification has on the global radiation budget. As mentioned, the implementation also includes improvements to CESM1's specified stratospheric aerosol SAD. The impact the new SAD forcing has on the chemical parameterisation of CESM1 is described in Tilmes et al. (2016).

Code and Input Data Availability

The original stratospheric aerosol dataset derived to force models participating in CCMI, that is the basis of the work presented here, is available from http://www.pa.op.dlr.de/CCMI/CCMI_SimulationsForcings.html.

Released CESM code is made available through a subversion repository. The code may be downloaded by following the specific "User's Guide" for each model version after registering as a CESM user. For more information please see: https://www2.cesm.ucar.edu/models/current. In addition to the latest CESM code, the latest version of the data used to create the optical parameters file as well as the final optical parameters files for CAMRT and RRTMG and stratospheric aerosol forcing file for CESM may be found within the input data repository (https://svn-ccsm-inputdata.cgd.ucar.edu/trunk/inputdata/). Access to this repository is managed similarly to the

CESM code repository and instructions for downloading data may also be found under each model's "User Guide" at https://www2.cesm.ucar.edu/models/current.

The scripts used to create the optical parameters for are attached in the supplement. All questions about these scripts should be directed to the lead author.

Acknowledgements

We thank Daniel Marsh, Rolando Garcia, Sean Santos and Michael Mills for their assistance in developing the new volcano parameterization. CESM is sponsored by the National Science Foundation (NSF) and the U.S. Department of Energy (DOE). Administration of the CESM is maintained by the Climate and Global Dynamics Division (CGD) at the National Center for Atmospheric Research (NCAR). Computing resources were provided by the Climate Simulation Laboratory at NCAR's Computational and Information Systems Laboratory (CISL), sponsored by the National Science Foundation and other agencies. Ryan R. Neely III was supported by the National Center for Atmospheric Research's Advanced Study Program (NCAR ASP) during this work.

References

Ammann, C. M., G. A. Meehl, W. M. Washington, and C. S. Zender: A monthly and latitudinally varying volcanic forcing dataset in simulations of 20th century climate, Geophys. Res. Lett., 30, 12, doi:10.1029/2003GL016875, 2003.

Arfeuille, F., Luo, B. P., Heckendorn, P., Weisenstein, D., Sheng, J. X., Rozanov, E., Schraner, M., Brönnimann, S., Thomason, L. W., and Peter, T.: Modeling the stratospheric warming following the Mt. Pinatubo eruption: uncertainties in aerosol extinctions, Atmos. Chem. Phys., 13, 11221-11234, doi:10.5194/acp-13-11221-2013, 2013.

Biermann, U. M., Luo, B.-P. and Peter, T.: Absorption spectra and optical constants of binary and ternary solutions of H2SO4, HNO3, and H2O in the mid infrared at atmospheric temperatures, J. Phys. Chem. A, 104(4), 783–793, doi:10.1021/jp992349i, 2000.

Canty, T., Mascioli, N. R., Smarte, M. D. and Salawitch, R. J.: An empirical model of global climate – Part 1: A critical evaluation of volcanic cooling, Atmos. Chem. Phys., 13(8), 3997–4031, doi:10.5194/acp-13-3997-2013, 2013.

Driscoll, S., Bozzo, A., Gray, L. J., Robock, A. and Stenchikov, G.: Coupled Model Intercomparison Project 5 (CMIP5) simulations of climate following volcanic eruptions, J. Geophys. Res, 117(D17), doi:10.1029/2012JD017607, 2012.

Eyring, V., Cionni, I., Bodeker, G. E., Charlton-Perez, A. J., Kinnison, D. E., Scinocca, J. F., Waugh, D. W., Akiyoshi, H., Bekki, S., Chipperfield, M. P., Dameris, M., Dhomse, S., Frith, S. M., Garny, H., Gettelman, A., Kubin, A., Langematz, U., Mancini, E., Marchand, M., Nakamura, T., Oman, L. D., Pawson, S., Pitari, G., Plummer, D. A., Rozanov, E., Shepherd, T. G., Shibata, K., Tian, W., Braesicke, P., Hardiman, S. C., Lamarque, J.-F., Morgenstern, O., Pyle, J. A., Smale, D. and Yamashita, Y.: Multi-model assessment of stratospheric ozone return dates and ozone recovery in CCMVal-2 models, Atmos. Chem. Phys, 10(19), 9451–9472, doi:10.5194/acp-10-9451-2010, 2010.

Eyring, V., and J.-F. Lamarque: Global Chemistry-Climate Modeling and Evaluation, Eos Trans. AGU, 93(51), 539, 2012.

Eyring, V., J.-F. Lamarque, P. Hess, F. Arfeuille, K. Bowman, M. P. Chipperfield, B. Duncan, A. Fiore, A. Gettelman, M. A. Giorgetta, C. Granier, M. Hegglin, D. Kinnison, M. Kunze, U. Langematz, B. Luo, R. Martin, K. Matthes, P. A. Newman, T. Peter, A. Robock, T. Ryerson, A. Saiz-Lopez, R. Salawitch, M. Schultz, T. G. Shepherd, D. Shindell, J. Stähelin, S.

Tegtmeier, L. Thomason, S. Tilmes, J.-P. Vernier, D. W. Waugh, and P. J. Young: Overview of IGAC/SPARC Chemistry-Climate Model Initiative (CCMI) Community Simulations in Support of Upcoming Ozone and Climate Assessments, SPARC Newsletter No. 40, p. 48-66, 2013.

Grainger, R. G.: Some Useful Formulae for Aerosol Size Distributions and Optical Properties, http://eodg.atm.ox.ac.uk/user/grainger/research/aerosols.pdf, last access: 2 Oct. 2015.

GISTEMP Team: GISS Surface Temperature Analysis (GISTEMP): NASA Goddard Institute for Space Studies, at http://data.giss.nasa.gov/gistemp/, last access: 11 Nov. 2015.

Haimberger, L., C. Tavolato, and S. Sperka: Towards elimination of the warm bias in historic radiosonde temperature records—Some new results from a comprehensive intercomparison of upper air data, J. Clim., 21, 4587–4606, 2008.

Hansen, J., R. Ruedy, M. Sato, and K. Lo: Global surface temperature change, Rev. Geophys., **48**, RG4004, doi:10.1029/2010RG000345, 2010.

Iacono, M., J. Delamere, E. Mlawer, M. Shephard, S. Clough, and W. Collins, Radiative forcing by long-lived greenhouse gases: Calculations with the AER radiative transfer models, J. Geophys. Res., 2008.

Jones, P. D., M. New, D. E. Parker, S. Martin, and I. G. Rigor: Surface Air Temperature and its Changes Over the Past 150 Years, Rev. Geophys., 37(2), 173—199, 1999.

Kay, J. E., C. Deser, A. Phillip, A. Mai, C. Hannay, G. Strand, J. Arblaster, S. Bates, G. Danabasoglu, J. Edwards, M. Holland, P. Kushner, J.-F. Lamarque, D. Lawrence, K. Lindsay, A. Middleton, E. Munoz, R. Neale, K. Oleson, L. Polvani, and M. Vertenstein: The Community Earth System Model (CESM) Large Ensemble Project: A Community Resource for Studying Climate Change in the Presence of Internal Climate Variability, Bulletin of the American Meteorological Society, doi: 10.1175/BAMS-D-13-00255.1, **96**, 1333-1349. http://journals.ametsoc.org/doi/abs/10.1175/BAMS-D-13-00255.1, 2015.

Kinnison, D. E., Brasseur, G. P., Walters, S., Garcia, R. R., Marsh, D. R., Sassi, F., Harvey, V. L., Randall, C. E., Emmons, L., Lamarque, J.-F., Hess, P., Orlando, J. J., Tie, X. X., Randel, W., Pan, L. L., Gettelman, A., Granier, C., Diehl, T., Niemeier, U. and Simmons, A. J.: Sensitivity of chemical tracers to meteorological parameters in the MOZART-3 chemical transport model, J. Geophys. Res, 112(D20), D20302, doi:10.1029/2006JD007879, 2007.

Knutson, T. R., Zeng, F. and Wittenberg, A. T.: Multimodel Assessment of Regional Surface Temperature Trends: CMIP3 and CMIP5 Twentieth-Century Simulations, Journal of Climate, 26(22), 8709–8743, doi:10.1175/JCLI-D-12-00567.1, 2013.

Kremser, S., et al. (2016), Stratospheric aerosol - Observations, processes, and impact on climate, Rev. Geophys., 54, doi:10.1002/2015RG000511.

Lamarque, J.-F., Emmons, L. K., Hess, P. G., Kinnison, D. E., Tilmes, S., Vitt, F., Heald, C. L., Holland, E. A., Lauritzen, P. H., Neu, J., Orlando, J. J., Rasch, P. J. and Tyndall, G. K.: CAM-chem: description and evaluation of interactive atmospheric chemistry in the Community Earth System Model, Geosci. Model Dev., 5(2), 369–411, doi:10.5194/gmd-5-369-2012, 2012.

Marsh, D. R., Mills, M. J., Kinnison, D. E., Lamarque, J.-F., Calvo, N. and Polvani, L. M.: Climate change from 1850 to 2005 simulated in CESM1 (WACCM), J. Climate, 26, 19, 1–65, doi:10.1175/jcli-d-12-00558.1, 2012.

Matzler: MATLAB Functions for Mie Scattering and Absorption Version 2, IAP Res. Rep, 1–26, 2002.

Meehl, G. A., Washington, W.M., Arblaster, J. M., Hu, A., Teng, H., Tebaldi, C., Sanderson, B., Lamarque, J. F. , Conley, A., Strand, W. G., and White III J. B.: Climate system response to external forcings and climate change projections in CCSM4. J. Climate, 25, 3661-3683, doi: http://dx.doi.org/10.1175/JCLI-D-11-00240.1, 2012.

Meehl, G. A., Washington, W. M., Arblaster, J. M., Hu, A., Teng, H., Kay, J. E., Gettelman, A., Lawrence, D. M., Sanderson, B. M. and Strand, W. G.: Climate change projections in CESM1(CAM5) compared to CCSM4, Journal of Climate, 26(17), 130306100525002–6308, doi:10.1175/JCLI-D-12-00572.1, 2013.

Mills, M. J., Schmidt, A., Easter, R., Solomon, S., Kinnison, D. E., Ghan, S. J., Neely, R. R., Marsh D. R., Conley, A., Bardeen, C. G., and Gettelman, A., Global volcanic aerosol properties derived from emissions, 1990–2014, using CESM1(WACCM), J. Geophys. Res. Atmos., 121, 2332–2348, doi:10.1002/2015JD024290, 2016.

Mlawer, E., S. Taubman, P. Brown, M. Iacono, and S. Clough, Radiative transfer for inhomogeneous atmospheres: RRTM, a validated correlated-k model for the longwave, J.

Geophys. Res., 102, 16663–16682, 1997.

Morice, C. P., Kennedy, J. J. and Rayner, N. A.: Quantifying uncertainties in global and regional temperature change using an ensemble of observational estimates: The HadCRUT4 data set, J. Geophys. Res., 117(D8), D08101, doi:10.1029/2011jd017187, 2012.

Neale, R. B., and co-authors: Description of the NCAR Community Atmosphere Model (CAM4.0), Tech. Rep. NCAR/TN-485+STR, National Center for Atmospheric Research, Boulder, CO, USA, 2010.

Neale, R. B., and co-authors: Description of the NCAR Community Atmosphere Model (CAM5.0), Tech. Rep. NCAR/TN-486+STR, National Center for Atmospheric Research, Boulder, CO, USA, 2012.

Neale, R. B., Richter, J., Park, S., Lauritzen, P. H., Vavrus, S. J., Rasch, P. J., and Zhang, M.: The Mean Climate of the Community Atmosphere Model (CAM4) in Forced SST and Fully Coupled Experiments, J. Climate, 2011.

Neely, R. R. I., Marsh, D. R., Smith, K. L., Davis, S. M. and Polvani, L. M.: Biases in southern hemisphere climate trends induced by coarsely specifying the temporal resolution of stratospheric ozone, Geophys. Res. Lett, 41(23), 8602–8610, doi:10.1002/2014GL061627, 2014.

Neely III, R.R. and Schmidt, A.: VolcanEESM: Global volcanic sulphur dioxide (SO2) emissions database from 1850 to present - Version 1.0. Centre for Environmental Data Analysis, doi:10.5285/76ebdc0b-0eed-4f70-b89e-55e606bcd568, 2016.

Newhall, C. and S. Self : The Volcanic Explosivity Index (VEI) - an Estimate of Explosive Magnitude for Historical Volcanism, J. Geophys. Res, 87(C2), 1231–1238, doi:10.1029/jc087ic02p01231, 1982.

Sato, M., Hansen, J. McCormick, P., and Pollack, J.: Stratospheric Aerosol Optical Depths, 1850-1990, J. Geophys. Res, 98(D12), 22,987–22,994, doi:10.1029/93jd02553, 1993.

Smith, T. M., Reynolds, R. W. and Peterson, T. C.: Improvements to NOAA's historical merged land-ocean surface temperature analysis (1880-2006), Journal of Climate, doi:10.1175/2007JCLI2100.1, 2008.

Solomon, S., Daniel, J. S., Neely, R. R., Vernier, J. P., Dutton, E. G. and Thomason, L. W.: The Persistently Variable "Background" Stratospheric Aerosol Layer and Global Climate Change, Science, 333(6044), 866–870, doi:10.1126/science.1206027, 2011.

SPARC CCMVal: SPARC CCMVal, SPARC CCMVal Report on the Evaluation of Chemistry-Climate Models, V. Eyring, T. G. Shepherd, D. W. Waugh (Eds.), SPARC Report No. 5, WCRP-X, WMO/TD-No. X, 2010.

Stenchikov, G. L., Kirchner, I., Robock, A., Graf, H.-F., Antuña, J. C., Grainger, R. G., Lambert, A. and Thomason, L.: Radiative forcing from the 1991 Mount Pinatubo volcanic eruption, J. Geophys. Res, 103(D12), 13837, doi:10.1029/98JD00693, 1998.

Taylor, K. E., Stouffer, R. J. and Meehl, G. A.: An Overview of CMIP5 and the Experiment Design, Bulletin of the American Meteorological Society, 93(4), 485–498, doi:10.1175/BAMS-D-11-00094.1, 2012.

Tilmes, S., Garcia, R. R., Kinnison, D. E., Gettelman, A. and Rasch, P. J.: Impact of geoengineered aerosols on the troposphere and stratosphere, Journal of Geophysical Research: Atmospheres, 114(D12), doi:10.1029/2008JD011420, 2009.

Tilmes, S., Lamarque, J.-F., Emmons, L. K., Kinnison, D. E., Marsh, D., Garcia, R. R., Smith, A. K., Neely, R. R., Conley, A., Vitt, F., Val Martin, M., Tanimoto, H., Simpson, I., Blake, D. R., and Blake, N.: Representation of the Community Earth System Model (CESM1) CAM4-chem within the Chemistry-Climate Model Initiative (CCMI), Geosci. Model Dev., 9, 1853-1890, doi:10.5194/gmd-9-1853-2016, 2016.

Tabazadeh, A., Toon, O. B., Clegg, S. L. and Hamill, P.: A new parameterisation of H2SO4/H20 Atmospheric implications, Geophys. Res. Lett, 24(15), 1931–1934, doi:10.1029/97gl01879, 1997.

Thompson, D. W. J., Wallace, J. M., Jones, P. D. and Kennedy, J. J.: Identifying Signatures of Natural Climate Variability in Time Series of Global-Mean Surface Temperature: Methodology and Insights, J. Clim., 22(22), 6120–6141, doi:10.1175/2009JCLI3089.1, 2009.

Wiscombe, W. J., Mie scattering calculations: Advances in technique and fast, vector-speed computer codes., Technical Report Tech. Note. NCAR/TN-140+STR, NCAR, 1996.

Xia, L., Robock, A., Tilmes, S., and Neely III, R. R.: Stratospheric sulfate geoengineering could enhance the terrestrial photosynthesis rate, Atmos. Chem. Phys., 16, 1479-1489, doi:10.5194/acp-16-1479-2016, 2016.

Zanchettin, D., Timmreck, C., Khodri, M., Robock, A., Rubino, A., Schmidt, A. and Toohey, M.: A coordinated modeling assessment of the climate response to volcanic forcing. *Past Global Changes Magazine*, *23*, pp.54-55, 2015.

Model Version	Radiative Transfer Model	Standard Aerosol Mass Input File	Mass Composiition Assumptions	Optical Properties Look Up Table	Optical Properties Dependencies	Size Distribution Assumptions	SAD File
CCSM4/CESM1(CAM4)	CAMRT	CCSM4_volcanic_1850-2008_prototype1.nc	75% H_2SO_4 + 25% H_2O with ρ =1750 kg/m^3 at 215K	sulfuricacid_cam3_c080918.nc	Spectral Band & Mass	Log-normal with Constant wet r_{eff} = 0.426 μm Constant σ(ln r) = 1.25	N/A
CESM1(WACCM4)	CAMRT	Computed from SAD	Kinnison et al. [2007] & Tabazadeh et al. [1997]	sulfuricacid_cam3_c080918.nc	Spectral Band & Mass	Constant wet r_{eff} = 0.5 μm Constant σ(ln r) = 1.25	SAD_SULF_1849-2100_1.9x2.5_c090817.nc
CESM1(CAM5)	RRTMG	CCSM4_volcanic_1850-2008_prototype1.nc	75% H_2SO_4 + 25% H_2O with ρ =1750 kg/m^3 at 215K	rrtmg_Bi_sigma1.8_c100521.nc	Spectral Band, r_g & Mass	Log-normal with r_g diagnosed from mass density Constant σ(ln r) = 1.8	N/A
CESM1(CAM4-chem-CCMI) and Newer Tags & CESM1(WACCM4-CCMI) and Newer Tags	CAMRT	CESM_1849_2100_sad_V3_c160211.nc	75% H_2SO_4 + 25% H_2O with ρ =1750 kg/m^3 at 215K	volc_camRT_byradius_sigma1.6_c130724.nc	Spectral Band, r_g & Mass	Log-normal with Varying r_g as specifed by input file Constant σ_g=1.6	Read from Standard Aerosol Mass Input File
CESM1(CAM5) and Newer Tags	RRTMG	CESM_1849_2100_sad_V3_c160211.nc	75% H_2SO_4 + 25% H_2O with ρ =1750 kg/m^3 at 215K	volc_camRRTMG_byradius_sigma1.6_c130724.nc	Spectral Band, r_g & Mass	Log-normal with Varying r_g as specifed by input file Constant σ_g=1.6	Read from Standard Aerosol Mass Input File

Table 1. Summary of the old (orange) and new (green) stratospheric aerosol prescription parameterizations in CESM1 model configurations.

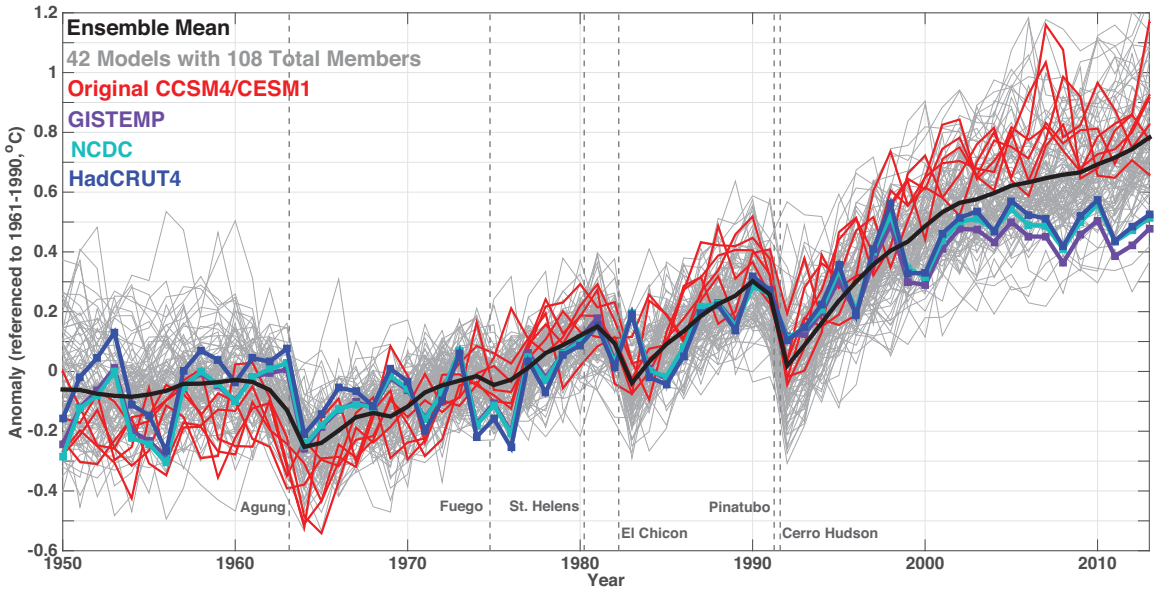

Figure 1. Global annual mean surface temperature anomalies from 1950 to 2013 referenced to the mean taken from 1961 to 1990. Light grey lines represent the 108 model members that contributed to the RCP4.5 scenario of CMIP5. The black line represents the multi-model ensemble mean. The members contributed by NCAR's CCSM4/CESM1 are highlighted in red. Three observational based datasets have been included for comparison: the GISS Surface Temperature Analysis (GISTEMP) in purple (Hansen et al., 2010; GISTEMP Team, 2015), NOAA's National Climatic Data Center's global surface temperature anomalies in teal (Jones et al. 1999; Smith et al., 2008) and global anomalies from the Hadley Centre of the UK Met Office (HADCRUT4) in blue (Morice et al., 2012).

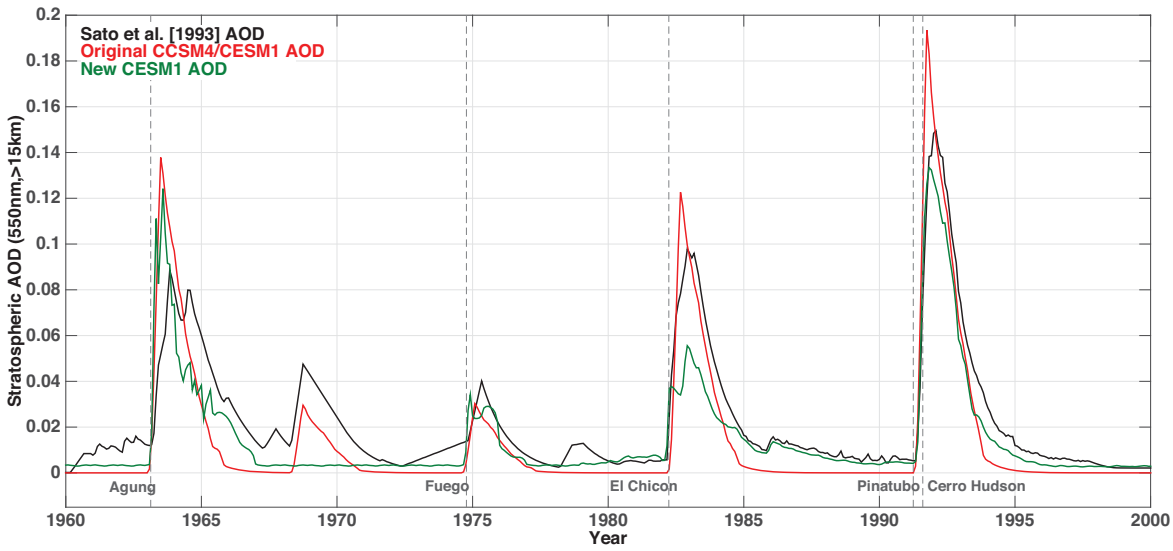

Figure 2. Globally averaged stratospheric AOD at 550 nm integrated from 15km and above. The red line represents the AOD as simulated by the original CCSM4/CESM1 simulation configurations. The green line represents the new AOD determined from the SAGE 4λ forcing file. For comparison, the latest AOD from the Sato et. al. (1993) dataset is shown in black.

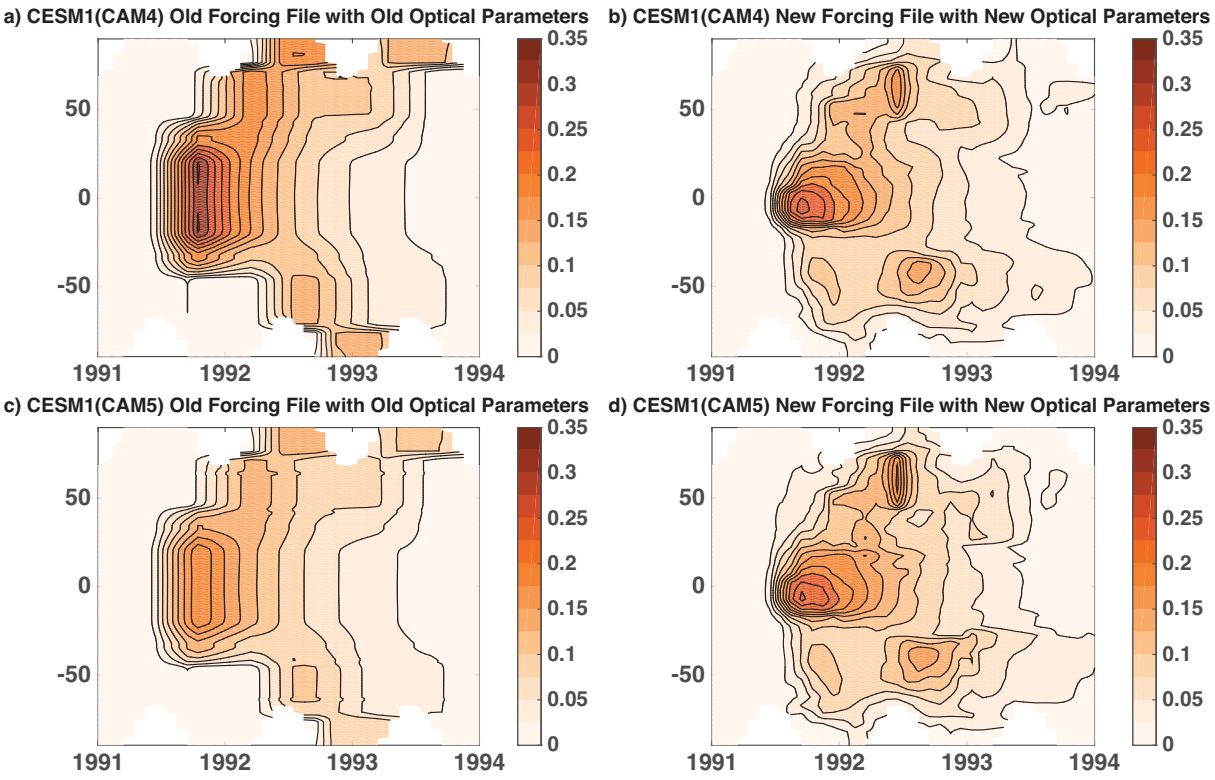

Figure 3. Monthly times series comparison of the zonal mean SAOD at 550 nm after the 1991 Mt. Pinatubo eruption for the old (panels a & c) and new (panels b & d) prescribed stratospheric aerosol scheme in CESM1(CAM4) (panels a & b) and CESM1(CAM5) (panels c & d). Results for CESM1(WACCM4) and CESM1(CAM4-Chem) are not shown as the new stratospheric aerosol are identical to those utilised in the new CESM1(CAM4) prescription.

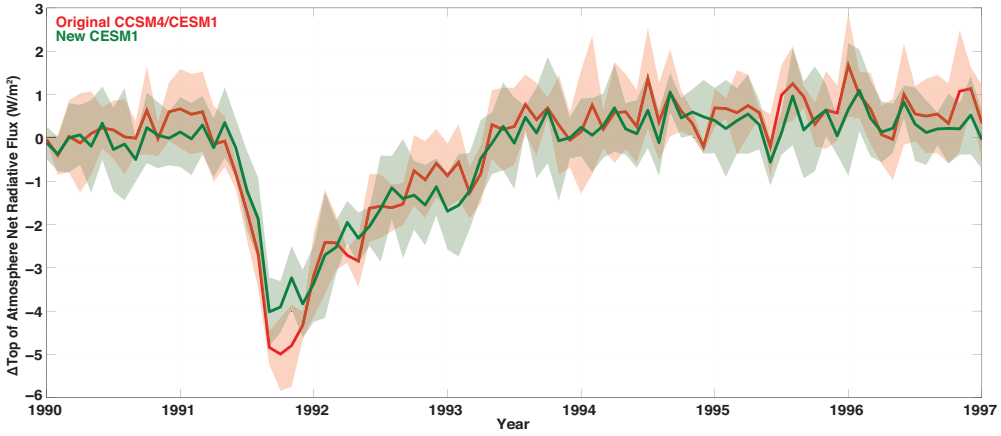

Figure 4. Global, monthly, ensemble, mean change in the top of atmosphere radiative flux due to the simulated Mt. Pinatubo eruption in June of 1991. Each original and new volcanic ensemble member is differenced from a set of simulations (not shown) conducted with identical initial conditions but with no stratospheric AOD forcing. Shaded regions represent $\pm 1\sigma$ standard deviation of the ensemble.

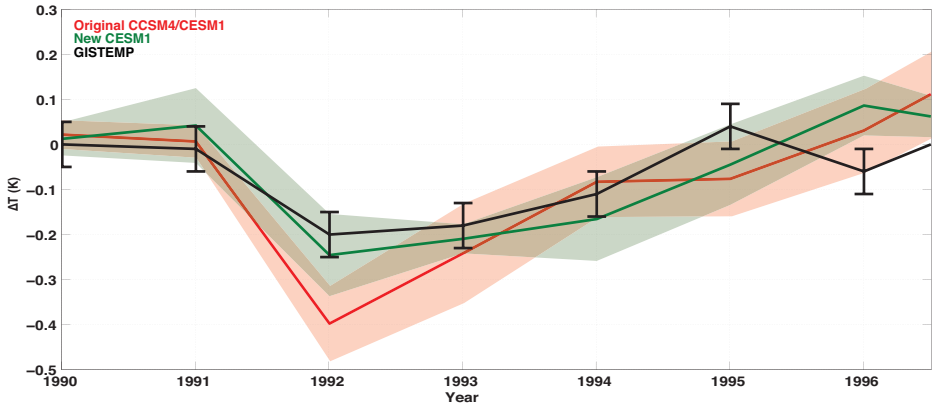

Figure 5. Global, annual, ensemble, mean temperature anomaly due to the observed (GISTEMP) and simulated Mt. Pinatubo eruption in June of 1991. Anomalies are referenced to the 1990 annual mean in each ensemble member. Shaded regions represent ±1σ standard deviation of the ensemble. Error bars on the observed record come from Hansen et al. (2010) and the GISTEMP Team (2015) estimates.

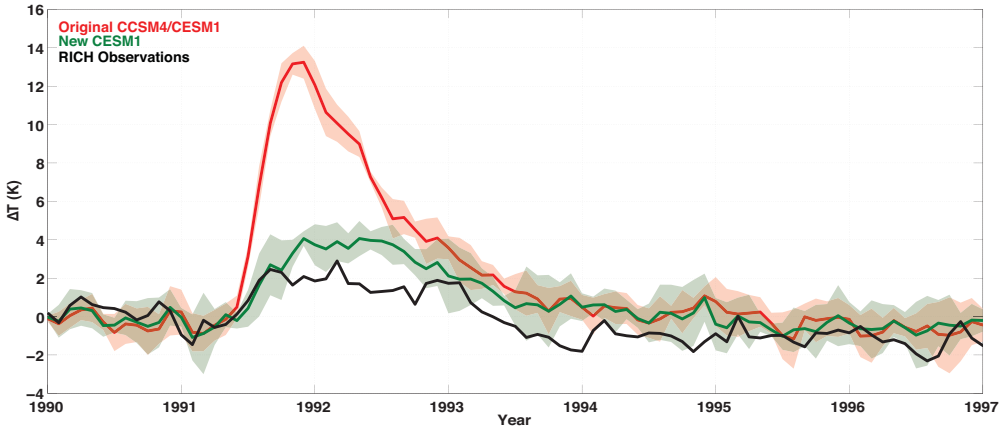

Figure 6. Tropical (20°S to 20°N), monthly, ensemble, mean temperature anomaly at 50hPa following the simulated Mt. Pinatubo eruption in June of 1991. Anomalies are referenced to the 1990 annual mean in each ensemble member. Shaded regions represent ±1σ standard deviation of the ensemble. The RICH data observations (black) come from Haimberger et al. (2008).